Electronic Supplementary Information

Inner Salt-Shaped Small Molecular Photosensitizer with Extremely Enhanced Two-Photon Absorption for Mitochondrial-Targeting Photodynamic Therapy

Wenbo Hu, Tingchao He, Rongcui Jiang, Jun Yin, Lin Li, Xiaomei Lu, Hui Zhao, Lei Zhang, Ling Huang, Handong Sun, Wei Huang and Quli Fan**

1. Experimental details

Materials: 2, 2-((2, 5-diiodo-1, 4-phenylene) bis (oxy)) bis (N, N-diethylethanamine) (monomer 2) was reported in our previous literature[1] and used as received. The methyl 4-ethynylbenzoate (monomer 1), 2, 2'-((2,5-diiodo-1,4-phenylene) bis (Oxy)) bis (N, N-diethylethanamine) (DBD), and 4, 4'-((2,5-bi's (2-(diethylamino) ethoxy) -1,4-phenylene) bis (ethyne-2,1-diyl)) dibenzoic acid (DBA) were synthesized according to the literature procedures.[1] N-acetyl-L-cysteine (NAC) and 2',7'-dichlorfluorescein-diacetate (DCFH-DA) was purchased from Sigma-Aldrich (St. Louis, MO, USA). Anti-PARP1 (9532), anti-cleaved Caspase-3 (Asp175), anti-β tubulin (ab6046) and HRP-conjugated secondary antibody (7074S) were purchased from abcam or Cell signal, respectively. Unless otherwise noted, all reagents were purchased from Sigma Aldrich and used without additional purification. All other solvents were purchased from either Fisher Scientific or Aldrich and used as received.

Characterization: NMR spectra were recorded on a Bruker Ultra Shield Plus 400 MHz spectrometer (^{1}H: 400 MHz, ^{13}C: 100 MHz) and referenced to tetramethylsilane (TMS) as the internal standard, the following abbreviations are used to explain the multiplicities: s=singlet, d=doublet, t=triplet, q=quartet, m=multiplet. Mass spectra were obtained on a matrix-assisted laser desorption/ionization time of flight mass spectrometry MS (MALDI-TOF, Bruker AutoFlex III system). Single-crystal X-ray crystallography was carried out on a Bruker SMART APEX-II CCD diffractometer equipped with graphite monochromated Mo-K radiation. The steady-state absorption data and photoluminescence spectra were measured by a Shimadzu UV-3600 ultraviolet-visible-near-infrared spectrophotometer and an RF-5301PC spectrofluorometer, respectively. The time-resolved emission spectra and lifetime were measured using an Edinburgh FLSP920 fluorescence spectrophotometer equipped with a picosecond pulsed semiconductor light (EPL375) and a microsecond flash-lamp (uF900), respectively. The absolute quantum yield measured using an Edinburgh FLSP920 fluorescence spectrophotometer equipped with an integrating sphere and a xenon lamp. Two-photon absorption cross sections of molecules were

measured by the Z-scan technique using home-built experimental setup.[2] The laser source is a Ti:sapphire system that produced 100 fs pulses at a repetition of 80 MHz. All images were acquired on Leica TCS SP5X Confocal Microscope System equipped with Leica HCX PL APO 63x/1.20 W CORR CS, 405 nm Diode laser, white laser (470 nm to 670 nm, with 1 nm increments, with 8 channels AOTF for simultaneous control of 8 laser lines, each excitation wavelength provides 1.5 mV), and Ti-Sapphire laser (~4 W at 800 nm) which corresponded to approximately 1% (~40 mW at 800 nm) average power in the focal plane. All the calculations were done with Gaussian09 program (Revision B.01).

Synthetic route for target molecule

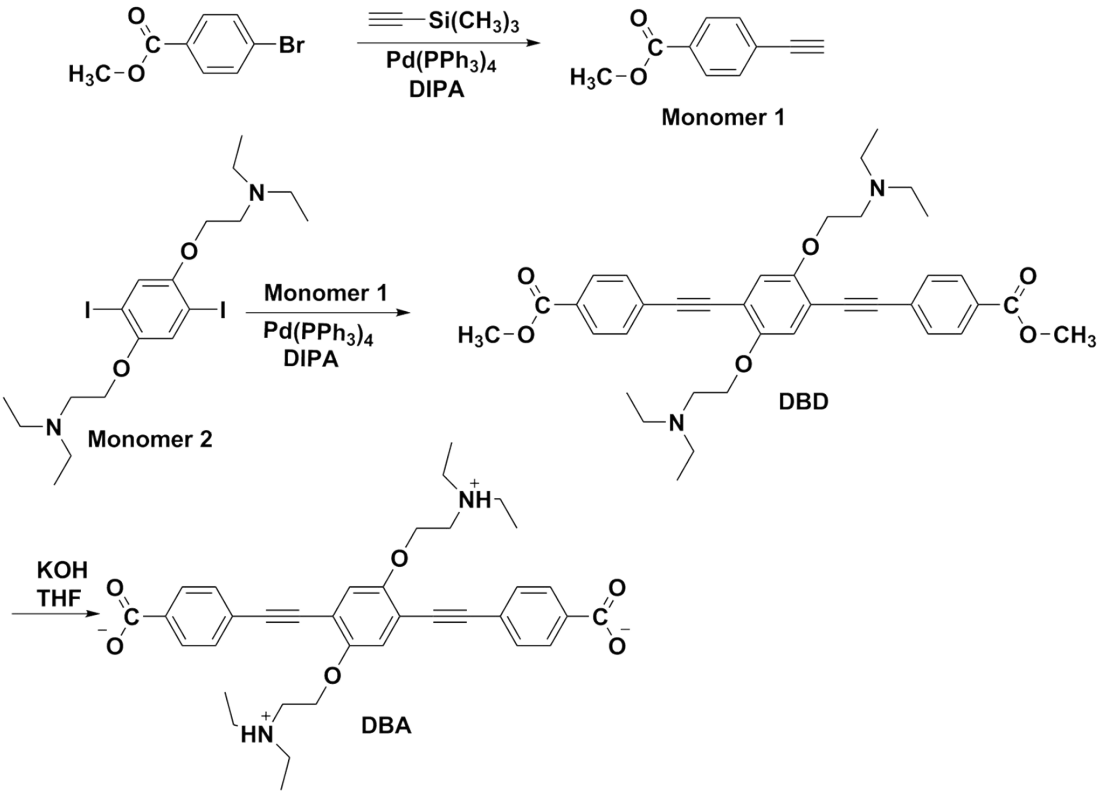

Fig.S1. Synthetic route of DBD and DBA.

Methyl 4-ethynylbenzoate (monomer 1)

A 2.1 g (10 mmol) sample of methyl 4-bromobenzoate, 0.55 g (0.5 mmol) of Pd $(PPh_3)_4$ and 0.112 g (0.6 mmol) of CuI were dissolved in 30 ml of diisopropylamine (DIPA). 5.6 ml (36 mmol) of (trimethylsilyl) acetylene was added into the vigorously stirred solution at room temperature for 30 min under nitrogen protection. The

reaction mixture was stirred at reflux for 24 h. After the mixture was filtered, the solvent was evaporated under reduced pressure; the residue was poured into 100 mL of water and extracted with chloroform three times. The organic layer was separated and washed with water three times and brine once and dried over $MgSO_4$. After the solvent was evaporated, the above mentioned compound was dissolved in 30 mL of THF and K_2CO_3 aqueous solution (4 g in 50 mL water) was added dropwise at room temperature and stirred for 60 min. After the stirring, the obtained light yellow organic layer was separated and the water layer was extracted with chloroform three times. The combined organic layers were washed with water twice and brine once and dried over $MgSO_4$. The mixture was filtered, the crude product was purified by chromatography using petroleum and the filtrate was evaporated by rotary evaporator to afford 1.3 g yellow crystals (yield 83.1%). ^{1}H NMR ($CDCl_3$, 400 MHz): 8.07 – 7.91 (m, 2H), 7.60 – 7.50 (m, 2H), 3.92 (s, 3H), 3.23 (s, 1H). ^{13}C NMR ($CDCl_3$, 100 MHz):165.94, 132.93, 129.54, 82.37,51.58. GC-MS (m/z): Calcd for $C_8H_{10}O_2$ [M]+, 160.1; found, 159.9.

4, 4-((2, 5-bis (2-(diethylamino) ethoxy)-1, 4-phenylene) bis (ethyne-2, 1-diyl)) dibenzoate (DBD)

A 0.5 g (3.1 mmol) sample of methyl 4-ethynylbenzoate, 0.8 g (1.4 mmol) 2,2'-((2,5-diiodo-1,4-phenylene) bis (Oxy)) bis (N, N-diethylethanamine) (monomer 2), 0.12 g (0.1 mmol) of Pd $(PPh_3)_4$, 0.052 g (0.2 mmol) Triphenylphosphane and 0.019 g (0.1 mmol) CuI were charged in a 250 mL round-bottom flask. Under nitrogen protection, added degaussed DIPA (30 mL) and THF (20 mL). The reaction mixture was stirred at reflux for 24 h under nitrogen protection. After removal of excess DIPA by rotary evaporation, the mixture was filtered, the combined organic layer was dried over anhydrous sodium sulfate, filtered and the solvent was removed by rotary evaporation. After removing the solvent, the residue was purified by chromatography using petroleum and dichloromethane (8:1) with triethylamine as the eluent. Remove eluent by rotary evaporation to give 0.7 g yellow powders (yield 78.5%). ^{1}H NMR ($CDCl_3$, 400 MHz): 8.09 – 7.97 (m, 4H), 7.63 – 7.53 (m, 4H), 7.04 (s, 2H), 4.11 (t, J = 5.9 Hz, 4H), 3.93 (s, 6H), 2.97 (t, J = 5.9 Hz, 4H), 2.68 (q, J = 7.1 Hz, 8H), 1.07 (t, J =

7.1 Hz, 12H). ^{13}C NMR ($CDCl_3$, 100 MHz): 166.57, 153.61, 131.46, 129.52, 128.03, 116.79, 113.74, 94.26, 88.92, 68.48, 52.27, 51.58, 48.00, 12.18. MALDI-TOF-MS (m/z): Calcd for $C_{38}H_{44}N_2O_6$ [M]+, 624.32; found: 624.40.

4,4'-((2,5-bis(2-(diethylamino)ethoxy)-1,4-phenylene)bis(ethyne-2,1-diyl))dibenzoic acid. (DBA)

The abovementioned compound (0.3 g, 0.5 mmol) was dissolved in 30 mL of dichloromethane and potassium hydroxide aqueous solution (4 g in 30 mL water) was added dropwise at room temperature and stirred for 60 min. After the stirring, the obtained water layer was separated and washed with dichloromethane three times. Diluted hydrochloric acid was added into water layer until the green precipitate not occur, the green precipitation was filtered and washed with water twice and brine once and dried over anhydrous sodium sulfate to give 0.25 g green powders (yield 87.2%). ^{1}H NMR (CD_3OD, 400 MHz): 8.05 (d, J = 8.4 Hz, 4H), 7.62 (d, J = 8.4 Hz, 4H), 7.35 (s, 2H), 4.52 – 4.45 (m, 4H), 3.74 – 3.67 (m, 4H), 3.42 (q, J = 7.3 Hz, 8H), 1.34 (q, J = 7.6 Hz, 12H). ^{13}C NMR (CD_3OD, 100 MHz): 152.94, 131.01, 129.52, 117.02, 113.94, 94.34, 64.27, 50.91, 48.74, 8.10. MALDI-TOF-MS (m/z): Calcd for $C_{36}H_{40}N_2O_6$ [M]+, 596.29; found: 596.45.

Theoretical model. The density functional theory (DFT) were performed to study the singlet geometries of neutral and anion states by exchange-correlation functional B3LYP and the unrestricted formalism (UB3LYP), respectively, together with basis sets 6-31G(d, p). All the optical transition matrix elements and corresponding excitation energies were calculated using time-dependent DFT (TD-DFT) based on range-separated functional CAM-B3LYP/6-31G(d, p) method. The solvation effects in methanol and THF used as solvents in the measurement were taken into account with the conductor-like polarizable continuum model (CPCM). For simulate the TPA cross sections, the lowest 100 excited states were taken account as the transition dipole moments for higher exited states are small. All the calculations were done with Gaussian09 program (Revision B.01).

The TPA process corresponds to simultaneous absorption of two photons. The TPA efficiency of an organic molecule, at optical frequency $\omega/2\pi$, can be

characterized by the TPA cross section δ(ω). It can be directly related to the imaginary part of the second hyperpolarizability $\gamma\left(-\omega_\sigma;\omega_1,\omega_2,\omega_3\right)$ by[3]

$$\delta(\omega)=\frac{3\hbar\omega^2}{2n^2c^2\varepsilon_0}Im\left[\gamma\left(-\omega_\sigma;\omega_1,\omega_2,\omega_3\right)\right]$$

where $\hbar\omega$ is the excitation energy, c is the speed of light, and ε_0 is the vacuum electric permittivity; n means the refractive index of the medium; ω_1, ω_2, and ω_3 are optical frequencies, and $\omega_\sigma=\omega_1+\omega_2+\omega_3$ is the polarization response frequency.

The two-photon transition matrix elements can be identified from the sum-over-states (SOS) formula, and the SOS equation for second hyperpolarizability γ is.[4]

$$\gamma_{ABCD}\left(-\omega_\sigma;\omega_1,\omega_2,\omega_3\right)$$

$$=\hat{P}\left[A\left(-\omega_\sigma\right),B\left(\omega_1\right),C\left(\omega_2\right),D\left(\omega_3\right)\right]\left(\begin{array}{l}\sum\limits_{i\neq0}\sum\limits_{j\neq0}\sum\limits_{k\neq0}\dfrac{\mu_{0i}^{A}\overline{\mu_{ij}^{B}\mu_{jk}^{C}}\mu_{k0}^{D}}{\left(\Delta_i-\omega_\sigma\right)\left(\Delta_j-\omega_2-\omega_3\right)\left(\Delta_k-\omega_3\right)}\\-\sum\limits_{i\neq0}\sum\limits_{j\neq0}\dfrac{\mu_{0i}^{A}\mu_{ij}^{B}\mu_{jk}^{C}\mu_{k0}^{D}}{\left(\Delta_i-\omega_\sigma\right)\left(\Delta_i-\omega_1\right)\left(\Delta_j-\omega_3\right)}\end{array}\right)$$

where A, B, C, and D are the molecular axes; 0 refer to the ground state and *i*, *j*, and *k* denote excited states; μ is the component of the dipole operator. To compare the calculated TPA cross section (δ) value with the experimental value measured in solution, the orientationally averaged value of γ is evaluated, which is

$$\gamma_{avg}=(1/5)\sqrt{\gamma_{xxxx}+\gamma_{yyyy}+\gamma_{zzzz}+\gamma_{xxyy}+\gamma_{yyzz}+\gamma_{yyxx}+\gamma_{zzxx}+\gamma_{zzyy}}$$

$^1O_2$ quantum yield measurement by detecting $^1O_2$ emission. One-photon excitation singlet oxygen generation was directly monitored by the characteristic emission of $^1O_2$ at ~1270 nm in D_2O solution. The $^1O_2$ emission was measured by using FluoroLog-3 spectrofluorometer (Jobin-Yvon) equipped with a more near-infrared sensitive photomultiplier (Hamamatsu model: DSS-IGA (1.9) 010L). An 850 nm long pass filter was placed before the detector. Considering the short phosphorescence luminescence (PL) lifetime of $^1O_2$ in water, the DBA solution was lyophilized. $TMPyP_4$ in D_2O was used as the reference (r), and Φ_r = 74% in water.[28] The $^1O_2$ quantum yield of the DBA can be calculated according to

$$\Phi_{DBA} = \Phi_r \times \frac{I_{DBA}}{I_r}$$

Where I_{DBA} and I_r represent the PL peak areas of $^1O_2$ produced by the DBA and $TMPyP_4$, respectively.

Procedure for cell imaging. Hela cells were seeded in glass-bottom dishes (Mattek) and grown till 70 ~ 80% confluency. Subsequently, cells were incubated with DBA (2 μM prepared in fresh media from a buffer stock) for 2 h, and then further incubated with 200 nM of the Mito-tracker. Cells were then washed three times with PBS, then imaged with the Leica TCS SP5X Confocal Microscope System. Images of DBA stained cells were collected at 420 ~ 500 nm by using a Ti-Sapphire laser excitation wavelength at 720 nm. Background signals of all images were verified to be nearly zero by imaging the same cells treated with a buffer control. MitoTracker® Red CMXRos dye was from Invitrogen (Ex = 550 nm, PMT range: 570 ~ 650 nm).

Subcellular fractions separation. Hela cells were seeded in 6-well plates and incubated at 37 ^oC with 5% CO_2 overnight. Before collection, cells were incubated with DBA (10 μM) for 2 h. The cell pellets were lysed in mitochondria isolation buffer (10 mM Tris-HCl, 0.3 M sucrose, 0.5 mM EDTA, pH 7.4) with proteinase inhibitors. To release mitochondria from the cells, the lysates were applied to 27G needle for 90 times till 90% cells were broken (as determined by visual inspection under a light microscope). The lysates were spun at 4 ^oC at 100 g for 5 min to remove unbroken cells. The supernatant was collected and spun at 4 ^oC at 8000 g for 20 min, giving rise to two different fractions (soluble and pellet). The mitochondrial fraction, now isolated in the pellet fraction, was further sonicated in lysis buffer (PBS with 1% SDS and proteinase inhibitors). The above soluble fraction, which contains mostly cytosolic cellular components, was tested alongside for comparison. Subsequently, the presence of DBA in the lysates from both the mitochondrial and cytoplasmic fractions were assessed on a Perkin-Elmer LS50 spectrofluorometer.

Cell viability. XTT colorimetric cell proliferation kit (Roche) was used to determine cell viability according to manufacturer's guidelines. Briefly, cells were

grown to 20 ~ 30% confluence (since they will reach ~90% confluence with 24 h in the absence of compounds) in 96-well plates. The medium was aspirated and then treated with media (0.1 mL) containing different amounts of DBA or $TMPyP_4$. After incubation for 24 h, proliferation was assayed by using the XTT colorimetric cell proliferation kit (Roche). A total of three replicas were performed.

Intracellular $^1O_2$ detection. Hela cells were cultured in confocal microscope dishes to 20~30% confluence in complete DMEM medium and cultured for 24 h. Then, the medium was aspirated, washed with PBS, treated with medium containing 20 μM **DBA** for 2 h, and then further incubated with 10 μM $^1O_2$ probe DCFH-DA. After incubation for 20 min, the cells were washed again and exposed under two-photon confocal laser at 750 nm for 5 min to generate $^1O_2$. The green fluorescent signals of DCF at 505 nm ~ 555 nm were captured under the irradiation at 488 nm by using laser confocal microscopy.

TP-PDT. Hela cells were grown to 20 ~ 30% confluence (since they will reach ~90% confluence with 24 h in the absence of compounds) in 96-well plates. The medium was aspirated and then treated with media (0.1 mL) containing 2 μM of DBA or $TMPyP_4$. After incubation for 24 h, cells were washed using PBS and re-cultured in a serum-containing DMEM medium. Each well was exposed to 1 kHz femtosecond laser irradiation at 750 nm with power density of ~1.0 W cm^{-2}. Cells after PDT treatments were further incubated for 24 h for apoptosis followed by the XTT assay of the cell proliferation. Cell experiments without DBA under the same experimental conditions were performed for direct comparison.

Western blotting assay. The cells in 96-well were directly lysed with 20 L 1× SDS loading buffer for Western blotting assay (1 : 1000 for primary antibody if there is no specific highlight), and resolved on SDS-PAGE and transferred onto a nitrocellulose membrane (Hybond ECL, Amersham Pharmacia Biotech). The membrane were then blocked with 25 mM Tris-HCl, pH 7.4, 137 mM NaCl, 2.68 mM KCl, and 0.05% Tween 20 containing 5% nonfat milk for 1 h at room temperature. Membranes were incubated with primary antibodies, such as, anti-PARP1, anti-Cleaved Caspase-3 and anti-Tublin (1:5000) shaking 4°C overnight. HRP conjugated secondary antibody

(1:1000) is added at room temperature for 1 h. The antibody-reactive bands are visualized by chemiluminescent detection (ECL western detection kit; Amersham Pharmacia Biotech).

Statistical analysis: The statistical analysis of the samples was undertaken using a Student's t-test, and *p*-values < 0.05 were considered statistically significant. All data reported are means ± standard deviations, unless otherwise noted.

2 Figure and Table

2.1 Characterization of inner salt-shaped DBA

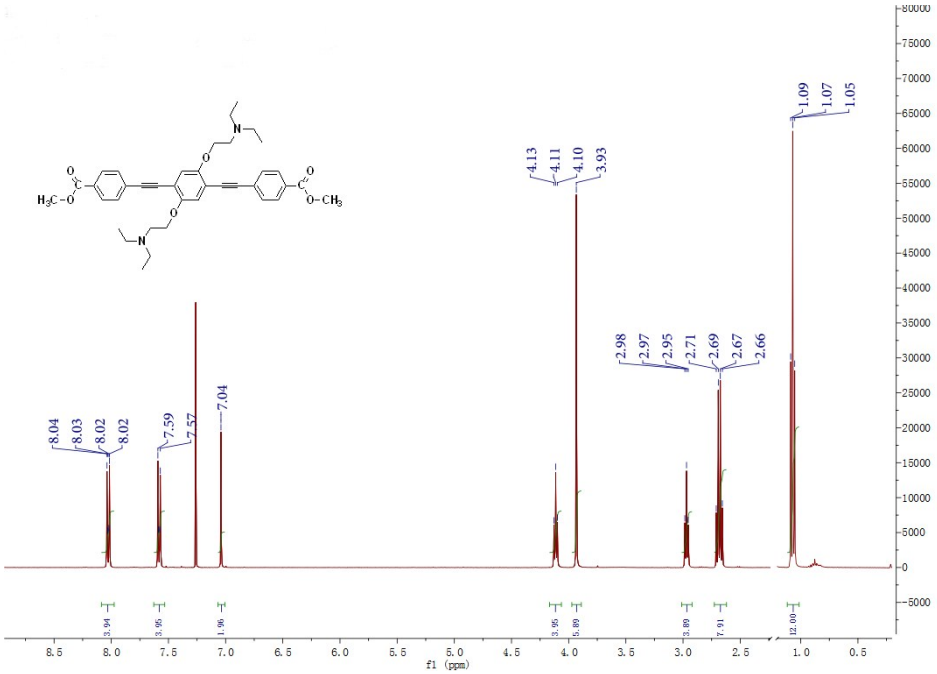

Fig.S2. ^{1}H NMR spectrum (400 MHz, 298 K) of DBD in Chloroform-*d* with concentration of 2 mM.

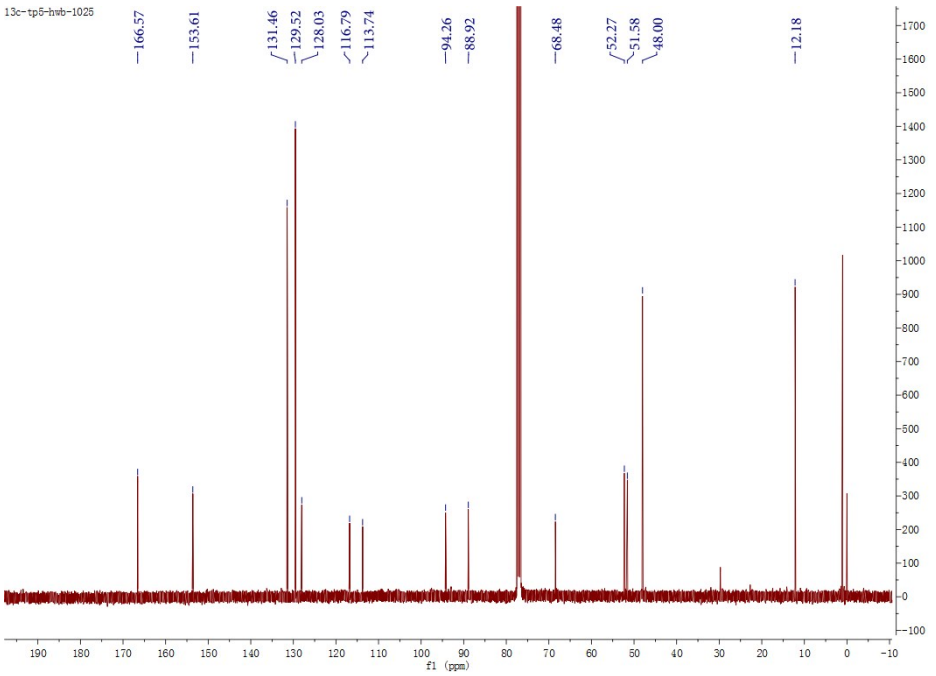

Fig.S3. ^{13}C NMR spectrum (100 MHz, 298 K) of DBD in Chloroform-*d* with concentration of 2 mM.

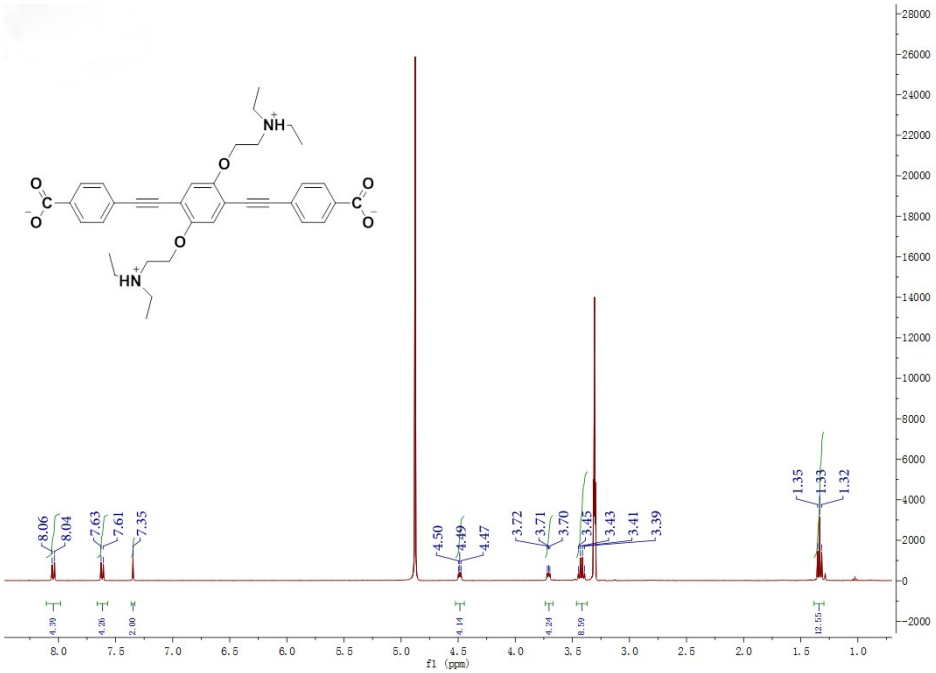

Fig.S4. ^{1}H NMR spectrum (400 MHz, 298 K) of DBA in Methanol-*d* with concentration of 2 mM. The absence of the peak at 3.93 (s, 6H) ppm in DBA indicating successfully de-methoxy while all signals corresponding to the nitrogen atoms shift to the lower field suggesting the formation of inner salt between carboxyl group and tertiary amine.

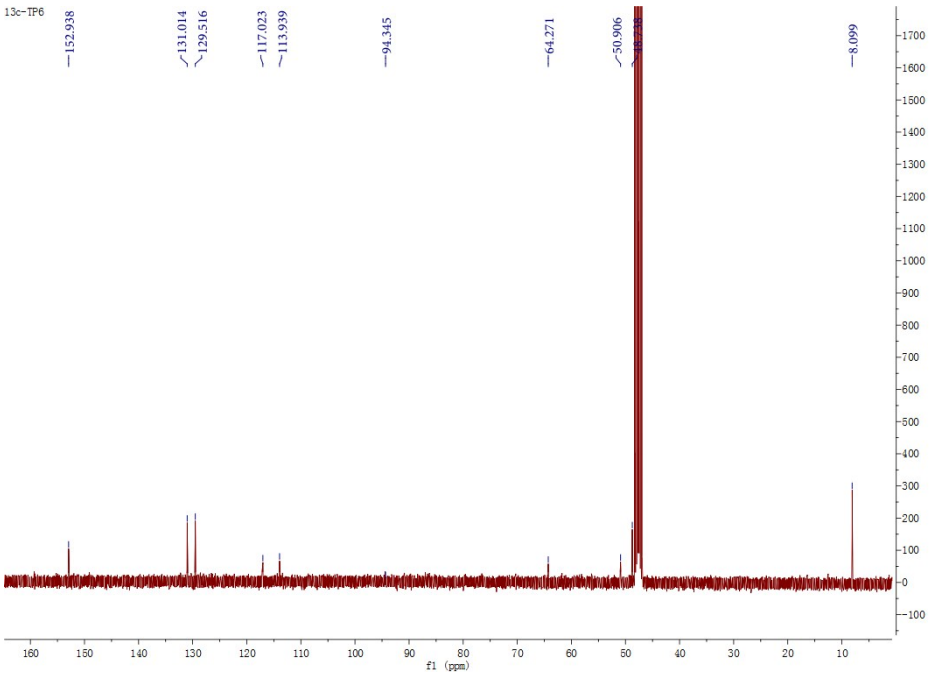

Fig.S5. ^{13}C NMR spectrum (100 MHz, 298 K) of DBA in Methanol-*d* with concentration of 2 mM.

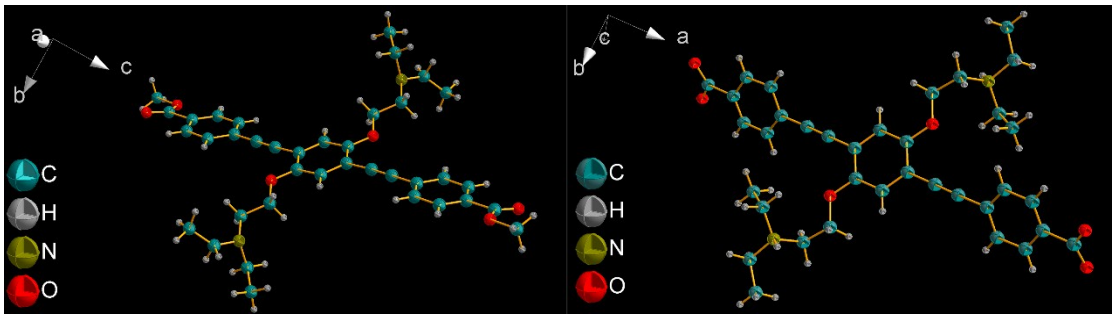

Fig.S6. Crystal structure diagrams of compound DBD (left) and DBA (right).

Table S1. Structure data of DBD and DBA single crystals.

Name	DBD	DBA
Formula	$C_{38}H_{44}N_2O_6$	$C_{36}H_{40}N_2O_6$
Wavelength (Å)	0.71073	1.54178
Space Group	P 21/n	P 4/n
Cell Lengths (Å)	a 6.156 (2), b 23.845 (10), c 12.467 (5)	a 31.236 (8), b 31.236 (8), c 8.080 (3)

Cell Angles (°)	α 90.00, β 100.292 (11), γ 90.00	α 90.00, β 90.00, γ 90.00
Cell Volume (Å3)	1800.4 (12)	7883.6 (4)
Z	2	8
Density (g/cm3)	1.152	1.005
F(000)	668.0	2544.0
h_{max}, k_{max}, l_{max}	7, 28, 14	35, 36, 9
T_{min}, T_{max}	0.979, 0.983	0.870, 0.942

The obtained crystal structures have been deposited at the Cambridge Crystallographic Data Centre and allocated the deposition number: 1409682 (DBD) and 1409683 (DBA).

The inner salt-shaped architecture of the DBA were studied by ^{1}H-NMR spectra and single-crystal X-ray diffraction. The ^{1}H-NMR spectrum of the DBD (**Fig.S2**) shows peak at 8.09 – 7.97 (m, 4H), 7.63 – 7.53 (m, 4H), and 7.04 (s, 2H), which correspond to the aromatic protons of the benzene ring. The peaks at 4.11 (t, J = 5.9 Hz, 4H), 2.97 (t, J = 5.9 Hz, 4H) is assigned to the alkyl protons between benzene ring and tertiary amine (-$OCH_2CH_2N(CH_2CH_3)_2$) and 2.68 (q, J = 7.1 Hz, 8H), 1.07 (t, J = 7.1 Hz, 12H) is assigned to the alkyl protons of methylene and methyl next to tertiary amine (-$CH_2N(CH_2CH_3)_2$). In **Fig.S4**, the peak at 3.93 (s, 6H) ppm is the characteristic peak of -OCH_3 next to the benzene ring which was disappear in DBA indicating the successfully de-methoxy. After the treatment of de-methoxyl, the DBA exhibited two well-resolved peaks at 3.74 – 3.67 (m, 4H) and 3.42 (q, J = 7.3 Hz, 9H) ppm corresponding to the methylene groups adjacent to nitrogen atoms (-$CH_2N(CH_2CH_3)_2$) and an peak at 1.34 (q, J = 7.6 Hz, 13H) assigned to the alkyl protons of methyl next to tertiary amine (-$CH_2N(CH_2CH_3)_2$). All signals corresponding to the nitrogen atoms shift to the lower field which arise from the deprotonation induced quaternized components,[1a, 5] suggesting the formation of inner salt. For a visual demonstration, In addition, single-crystal X-ray diffraction of DBA (**Fig.S6**) give a visual demonstration of inner salt-shaped architecture, in which once existed proton in carboxyl group was transfer to tertiary amine.

2.2 Room-temperature OP-related optical properties investigation

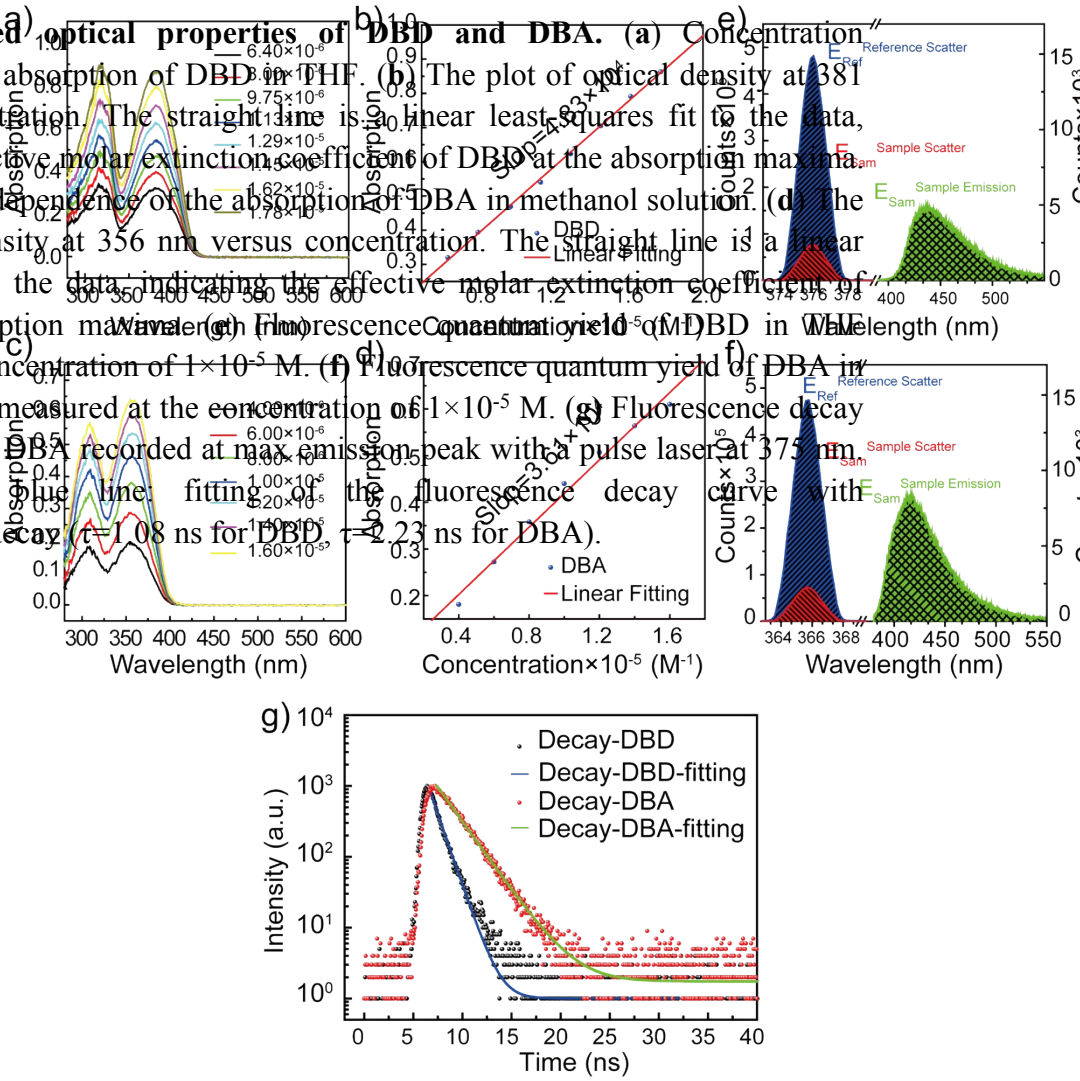

Fig.S7. **OP-related optical properties of DBD and DBA.** (**a**) Concentration dependence of the absorption of DBD in THF. (**b**) The plot of optical density at 381 nm versus concentration. The straight line is a linear least-squares fit to the data, indicating the effective molar extinction coefficient of DBD at the absorption maxima. (**c**) Concentration dependence of the absorption of DBA in methanol solution. (**d**) The plot of optical density at 356 nm versus concentration. The straight line is a linear least-squares fit to the data, indicating the effective molar extinction coefficient of DBA at the absorption maxima. (**e**) Fluorescence quantum yield of DBD in THF measured at the concentration of 1×10^{-5} M. (**f**) Fluorescence quantum yield of DBA in methanol solution measured at the concentration of 1×10^{-5} M. (**g**) Fluorescence decay curve of DBD and DBA recorded at max emission peak with a pulse laser at 375 nm. Green line and blue line: fitting of the fluorescence decay curve with monoexponential decay (τ=1.08 ns for DBD, τ=2.23 ns for DBA).

Table S2. OP-related optical properties of DBD and DBA.

Material	Solvent	λ_{ex}[a] [nm]	λ_{em}[b] [nm]	ε[c] [$M^{-1}cm^{-1}$]	φf[d]	τ[e] [ns]
DBD	THF	320,381	440	4.83×10^4	9.9%	1.08
DBA	Methanol	309,356	420	3.61×10^4	26.4%	2.23

[a] One-photon absorption maxima; [b] One-photon emission maxima; [c] Molar extinction coefficient at the absorption maxima (381nm for DBD, 356 nm for DBA) given in units of 1×10^{-5} M; [d] Fluorescence quantum yield measured at the concentration of 1×10^{-5} M; [e] Fluorescence lifetimes.

The OP-related optical properties were summarized in Table S2. **Fig.S7a** and **b** present the concentration-dependent absorption spectra of DBD and DBA, and both DBD and DBA exhibit consequently enhanced absorption with increasing concentration. **Fig.S7b** and **d** show there is a good linear relation between absorption and concentration. Based on Lambert Beers Law, we calculated the molar extinction coefficients (ε) of DBD and DBA at absorption maxima to be 4.83×10^4 $M^{-1}cm^{-1}$ and 3.61×10^4 $M^{-1}cm^{-1}$, respectively (**Fig.S7b,d**). Such measured ε of DBA is one order magnitude larger than existing PS, for example Photofrin with ε of 1.17×10^3 $M^{-1}cm^{-1}$,[6] and thus avoids high concentrations of PSs and light to be delivered to the tumour, which offers tremendous potential in practical bioapplications. Fluorescence quantum yield (φ_f) is a key parameter for fluorescent contrast for bioimaging. Here we employed an Edinburgh FLSP920 fluorescence spectrophotometer equipped with an integrating sphere to measure the absolute fluorescence quantum yield of DBD and DBA. As shown in Fig.S7e and f, the φ_f was measured based on:

$$\varphi_f = \frac{E_{Sam}^{Sample\ \ emission}}{E_{Ref}^{reference\ scatter} - E_{Sam}^{Sample\ \ Scatter}}$$

The calculated φ_f of DBD in THF and DBA in methanol is 9.9% and 26.4%, respectively. The fluorescence emission decay curve shown in **Fig.S7g** for DBD in THF and DBA in methanol, was measured by laser excitation at 375 nm. The blue and green line show a monoexponential decay curve fitted with a decay constant of

1.08 ns for DBD and 2.23 ns for DBA, indicative of only one existing species for DBD or DBA in its exited state.

2.3 Verification of two-photon absorption process

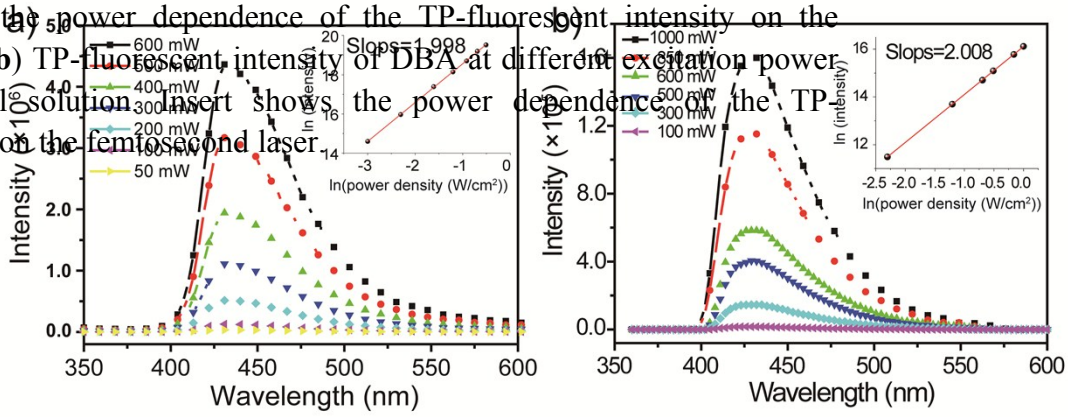

Fig.S8. (**a**) TP-fluorescent intensity of DBD at different excitation power density in THF. Insert shows the power dependence of the TP-fluorescent intensity on the femtosecond laser. (**b**) TP-fluorescent intensity of DBA at different excitation power density in methanol solution. Insert shows the power dependence of the TP-fluorescent intensity on the femtosecond laser.

To further determine the number of photons involved in such nonlinear process, the intensities of the emissions at 420 nm are recorded as a function of the excitation power density in ln-ln plots based on the following equation:[2b]

$$\ln\left(\boldsymbol{I}_{em}\right)=\mathbf{B}+\mathbf{n}\times\ln\left(\boldsymbol{I}_{ex}\right) \qquad \textbf{Equation. 1}$$

Here, I_{em} and I_{ex} are the emission and excitation intensities of TPA molecules, respectively. B is a constant and n is the number of photons involved in the multi-photon energy upconversion process. Insert in **Fig.S8a and b** show the fluorescence emission intensity increases along the excitation power density at 720 nm femtosecond laser. From the equation, the number of photons involved for this upconversion process were calculated to be 1.998 for DBD and 2.008 for DBA, respectively, which proves the TPA process.

2.4 Exclusion of linear absorption for DBA in two-photon absorption region

Fig.S9. Transmission spectra of DBD in THF and DBA in methanol.

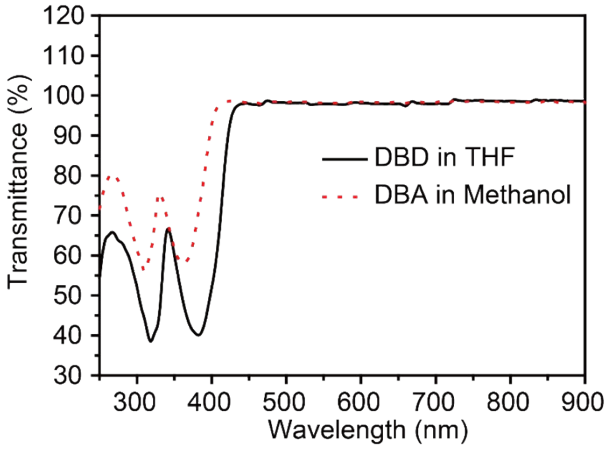

To exclude the influence of linear absorption of DBA in methanol or DBD in THF, the transmission spectra for DBA in methanol or DBD in THF were measured. Both samples have negligible linear absorption in the biological tissue transparency window of 650 - 800 nm (**Fig.S9**), excluding the influence of linear absorption of samples and solvent.

2.5 Triplet lifetime of DBA

Fig.S10. Luminescence decay curve (red line) of DBA monitored at 480 nm under oxygen-free environment with an excitation of 375 nm. Green line: fitting of the fluorescence decay curve. Fit=A+B1exp (-τ/τ_1)+B2exp (-τ/τ_2), τ_1=1.32 μs, τ_2=10.85 μs).

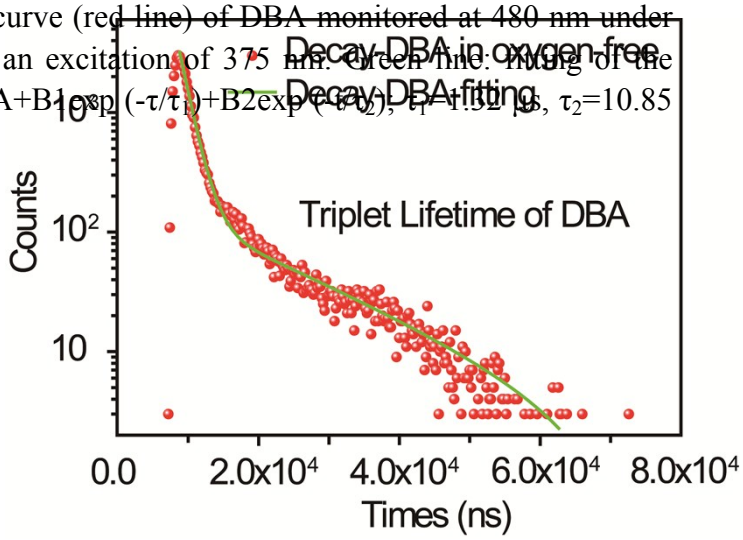

The triplet excited state lifetime was also evaluated to be 10.85 μs (70%) and 1.32 μs (30%) from the fitting of the emission decay as shown in **Fig.S10**, which is long enough to interact with molecular oxygen to yield $^1O_2$.

2.6 Feasibility of DBA for bioapplications

Fig.S11. (**a**) Dark-cytotoxicity of Hela cells after incubation with DBA of different concentrations for 24 h. (b) DBA in PBS and serum solutions were recorded after centrifugation at 6000 rpm for 5 min. No obvious precipitation was observed suggesting the excellent biocompatibility in both PBS and serum.

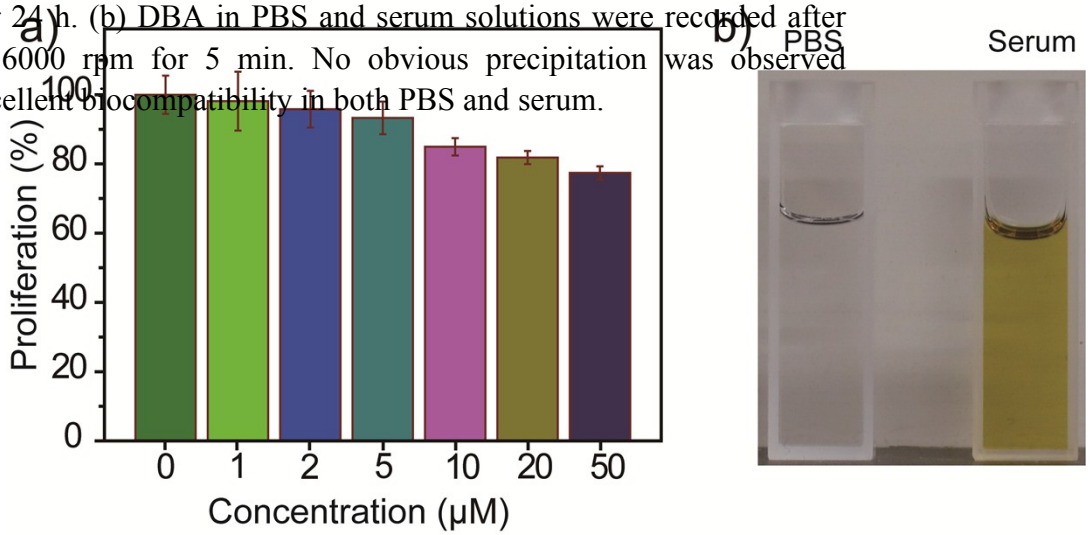

The XTT colorimetric cell proliferation kit was employed to determine the dark-cytotoxicity of DBA. No significant cytotoxicity was observed in **Fig.S11a** even when the concentration of DBA increased to 50 μM, implying super low dark-cytotoxicity. Meanwhile, the biocompatibility was also investigated through a typical protocol in which DBA soluble in PBS and serum solutions were recorded after centrifugation at 6000 rpm for 5 min (Hyclone was diluted in PBS to prepare serum solution).[7] No obvious precipitation was observed suggesting the excellent biocompatibility in both PBS and serum (**Fig.S11b**).

2.7 Chemical stability of DBA

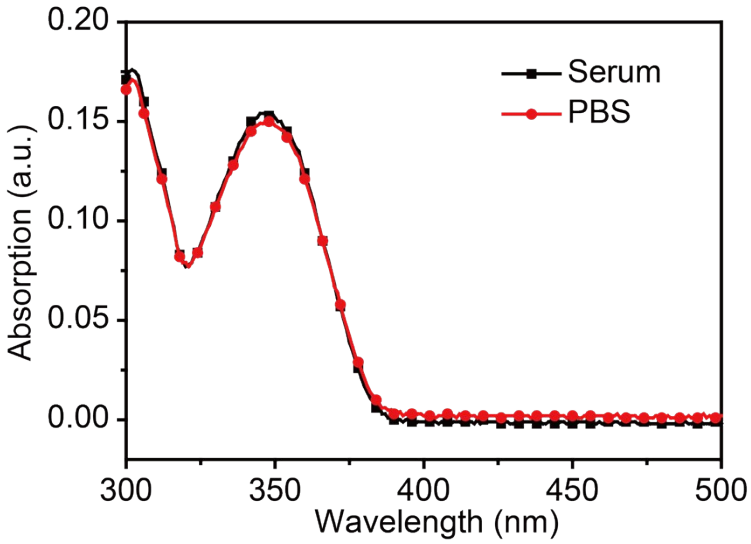

Fig.S12. The absorption spectra of 1.0 μM DBA in PBS buffer (pH 7.5) with/without 10 % serum labeled as PBS/Serum, respectively. No obvious spectral changes indicate the excellent chemical stability in physiological environment.

2.8 Optical interference between DBA and MTR

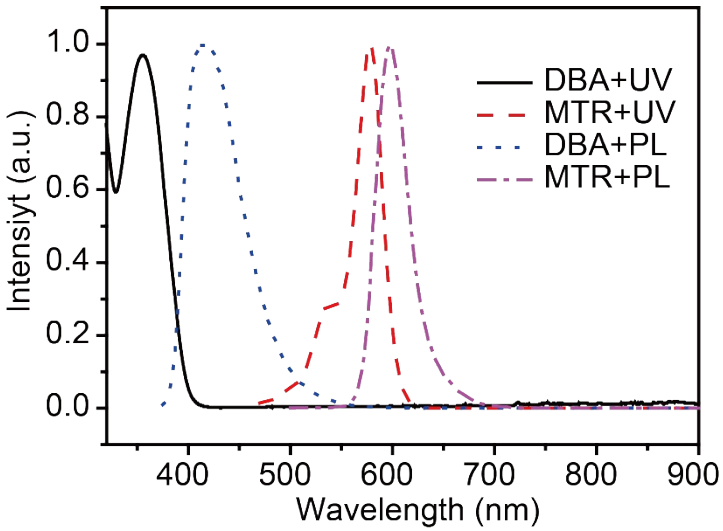

Fig.S13. The UV-absorption and PL spectra of DBA and MTR. The negligible overlap between absorption of MTR and fluorescence of DBA excludes the disturb influence.

To unambiguously determine the mitochondrial-targeting of DBA, a standard co-staining experiment was performed with DBA and a commercial probe (MTR), while the prerequisite of co-localization experiment is that no optical and chemical interferences exist between two dyes. As such, the absorption and fluorescence

properties of DBA and MTR were carefully studied and the final results demonstrate that DBA and MTR negligibly disturbed each other (**Fig.S13**).

2.9 Isoelectronic point (pI) estimation

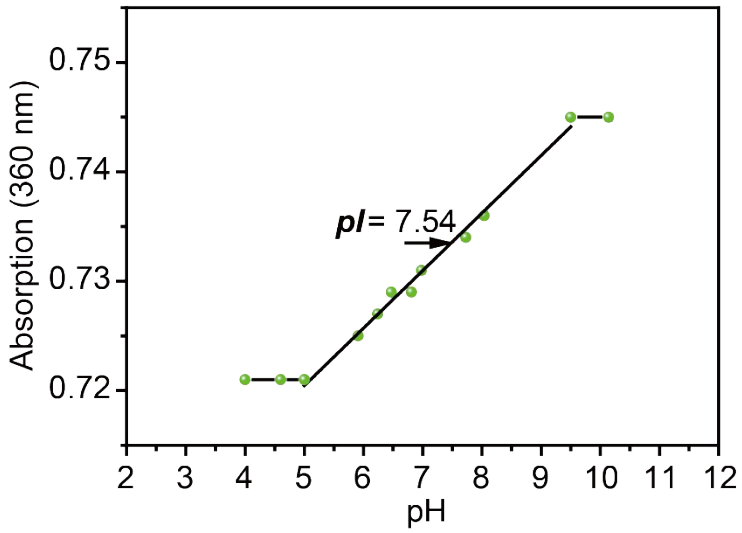

Fig.S14. The pH-dependent adsorption profiles of DBA, The arrow indicates the isoelectric point of DBA. The isoelectric point at 7.54 assure the positive-charged state of DBA in biological condition.

The key to target mitochondria is the electrostatic interactions between positive-charged mitochondrial-targeting groups and negative-charged membrane of mitochondria. Therefore, the isoelectronic point (*pI*) of DBA was measured via pH-dependent binding analysis,[8] in which strong ions exchanger (SP-Sephadex A-50) was utilized due to the fact that its capacity is constant over a much wider pH range than are those of the weak ones.[9] Two plateaus were seen in **Fig.S14**. The lower one represents the pH range where DBA carry the charge with the same sign as that of the ion exchanger and therefore remain unbound in the supernatant. The higher one represents the region where DBA are totally bound to the ion exchanger. The inflection reflects the change of the binding affinity of DBA due to the change of its charge characteristic. The midpoint of the transition is considered to be the isoelectric pH for DBA where there is no overall net charge on the DBA. In particular, the evaluated *pI* of 7.54 in **Fig.S14**, whether in a normal cell (pH = 6.8 - 7.2) or tumor

environment (pH = 6.5 - 6.8),[10] affords DBA weak positive-charged state, providing a high possibility to target mitochondria.

2.10 Reactive oxygen species generation in intracellular environment

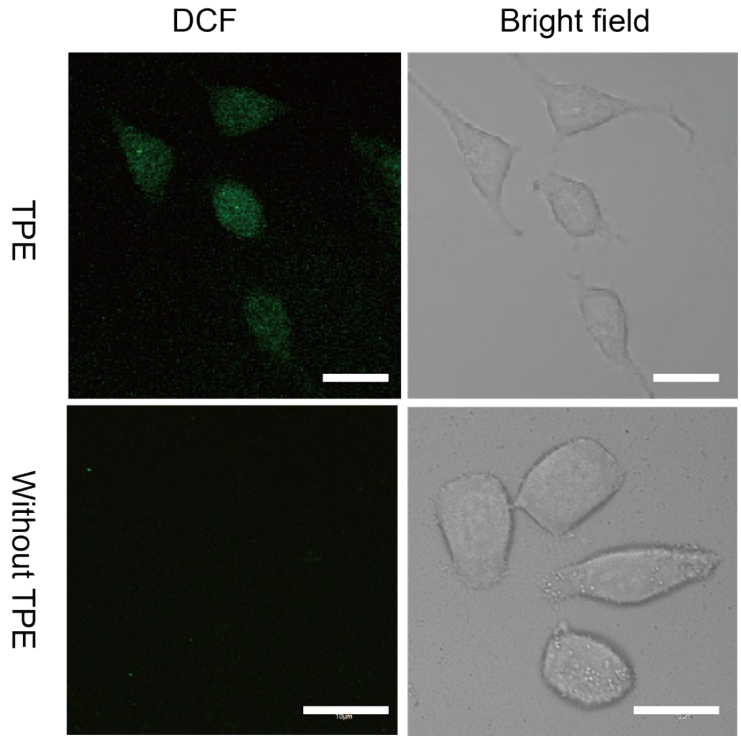

Fig.S15. Micrographs of reactive oxygen species generation in HeLa cells co-incubated with DBA and DCFH-DA with or without a two-photon confocal laser (750 nm) irradiation. The obvious green fluorescence of DCF in Hela cells after TPE compared to that without TPE demonstrates the reactive oxygen species (e.g., $^1O_2$) generation of DBA in intracellular environment.

3 References

[1] Q. L. Fan, Y. Zhou, X. M. Lu, X. Y. Hou, W. Huang, *Macromolecules* **2005**, *38*, 2927-2936.

[2] a) T. He, P. C. Too, R. Chen, S. Chiba, H. Sun, *Chem.--Asian J.* **2012**, *7*, 2090-2095; b) T. He, Z. B. Lim, L. Ma, H. Li, D. Rajwar, Y. Ying, Z. Di, A. C. Grimsdale, H. Sun, *Chem.--Asian J.* **2013**, *8*, 564-571.

[3] D. Beljonne, W. Wenseleers, E. Zojer, Z. Shuai, H. Vogel, S. J. K. Pond, J. W. Perry, S. R. Marder, J. L. Brédas, *Adv. Funct. Mater.* **2002**, *12*, 631-641.

[4] a) K. Sasagane, F. Aiga, R. Itoh, *J. Chem. Phys.* **1993**, *99*, 3738-3778; b) T. Lu, F. Chen, *J. Comput. Chem* **2012**, *33*, 580-592.

[5] B. Liu, W. L. Yu, Y. H. Lai, W. Huang, *Macromolecules* **2002**, *35*, 4975-4982.

[6] D. E. J. G. J. Dolmans, D. Fukumura, R. K. Jain, *Nat. Rev. Cancer* **2003**, *3*, 380-387.

[7] a) W. Hu, X. Lu, R. Jiang, Q. Fan, H. Zhao, W. Deng, L. Zhang, L. Huang, W. Huang, *Chem. Commun.* **2013**, *49*, 9012-9014; b) Z. Liu, J. T. Robinson, X. Sun, H. Dai, *J. Am. Chem. Soc.* **2008**, *130*, 10876-10877.
[8] R. N. Farías, A. E. López Viñals, E. Posse, R. D. Morero, *Anal. Biochem.* **1989**, *264*, 285-287.
[9] V. C. Yang, R. Langer, *Anal. Biochem.* **1985**, *147*, 148-155.
[10] M. Stubbs, P. M. J. McSheehy, J. R. Griffiths, C. L. Bashford, *Mol. Med. Today* **2000**, *6*, 15-19.